Journal of
Analytical & Bioanalytical Techniques

Trivedi et al., J Anal Bioanal Tech 2015, 6:4
DOI: 10.4172/2155-9872.1000256

Research Article Open Access

Thermal and Physical Properties of Biofield Treated Bile Salt and Proteose Peptone

Mahendra Kumar Trivedi[1], Shrikant Patil[1], Rakesh K. Mishra[2] and Snehasis Jana[2*]

[1]*Trivedi Global Inc., 10624 S Eastern Avenue Suite A-969, Henderson, NV 89052, USA*

[2]*Trivedi Science Research Laboratory Pvt. Ltd., Hall-A, Chinar Mega Mall, Chinar Fortune City, Hoshangabad Rd., Bhopal-462026, Madhya Pradesh, India*

Abstract

Bile salt (BS) and proteose peptone (PP) are important biomacromolecules being produced inside the human body. The objective of this study was to investigate the influence of biofield treatment on physicochemical properties of BS and PP. The study was performed in two groups (control and treated). The control group remained as untreated, and biofield treatment was given to treated group. The control and treated BS and PP samples were characterized by particle size analyzer (PSA), Brunauer-Emmett-Teller (BET) analysis, differential scanning calorimetry (DSC), x-ray diffraction (XRD), and thermogravimetric analysis (TGA). PSA results showed increase in particle size (d_{50} and d_{99}) of both treated BS and PP as compared to control. Surface area analysis showed minimal decrease by 1.59%, in surface area of treated BS as compared to control. However, the treated PP showed increase (8%) in surface area as compared to control. DSC characterization showed increase in melting temperature of treated BS as compared to control. Whereas, DSC thermogram of treated PP showed decrease in melting temperature with respect to control. Moreover, the DSC of control and treated PP showed presence of exothermic peaks which were possibly due to protein aggregation. The treated PP showed higher exothermic transition temperature as compared to control. XRD analysis revealed slight reduction in crystalline nature of BS as compared to control. On the other hand, XRD data of control and treated PP showed an amorphous nature. TGA analysis of treated BS showed maximum thermal decomposition temperature at 22°C which was higher as compared to control sample (106°C). This could be due to biofield treatment which may enhance the thermal stability of treated BS with respect to control. However, the TGA thermogram of treated PP showed decrease in maximum thermal stability as compared to control. The overall results showed that biofield treatment has significantly altered the physical and thermal properties of BS and PP.

Keywords: Bile salt; Proteose peptone; Particle size; Brunauer-Emmett-Teller analysis; X-ray diffraction; Differential scanning calorimetry; Thermogravimetric analysis

Abbreviations: PSA: Particle Size Analyzer; BET: Brunauer-Emmett-Teller analysis; DSC: Differential Scanning Calorimetry; XRD: X-ray Diffraction; TGA: Thermogravimetric Analysis; DTA: Differential Thermal Analyzer; DTG: Derivative Thermogravimetry; BS: Bile Salt; PP: Proteose Peptone

Introduction

Bile salts (BS) are commonly known as bio-surfactants that plays crucial physiological role in human gastro intestinal tract such as fat digestion and absorption of nutrients and also serve as a mean for removal of waste products from blood [1,2]. Briefly, BS acts as a carrier for fat soluble products due to its ability of forming micelles with phospholipids. Moreover, the BS plays an important role in nutrition by improving solubility and transport of fat soluble nutrients to the mucosa of small intestine. Based on chemical nature of BS are flat molecules with both hydrophilic and hydrophobic faces [3]. Many literature reports provided interesting information about the self-assembly nature of BS in solution suggesting the fascinating properties of BS aggregates as compared to conventional surfactants [4-6]. Due to this micellar nature of BS, which enables solubilization and transport of lipid soluble compounds thus it helps in fat digestion. Therefore, this same biological function can be exploited for pharmaceutical application since most drugs currently in development have low water solubility [1]. Thus BS based carrier systems are promising for specific targeting and absorption of non-soluble compounds. However, it was shown that BS is a poor surface active-agent compared to other commonly used surfactants such as dodecyl sulfate and sodium dodecanoate. Hence, in order to improve these properties BS should be modified in order to confer better physicochemical properties.

On the other hand proteose peptone (PP) is obtained from bovine milk which is partially consist of a number of heat stable minor proteins, glycoproteins, and largely of casein derived peptides [7,8]. These are generated in human body by the action of proteinases (mainly plasmin) of all the four main casein proteins [9-11]. These protein compounds require proper modification in order to alleviate its properties which can be utilized for further applications.

Scientists have demonstrated that short lived electrical events or action potential occurs in several types of mammalian cells such as neurons, muscle cells, and endocrine cells [12]. For example, the cells in the nervous system communicate with each another by means of electrical signals that travel along the nerve processes. Therefore, it is hypothesized that biofield exists around the human body and the evidence can be found using medical technologies such as Electromyography, Electrocardiography and electroencephalogram [13].

Thus, human has the ability to harness the energy from environment or universe and can transmit into any living or nonliving

***Corresponding authors:** Snehasis Jana, Trivedi Science Research Laboratory Pvt. Ltd., Hall-A, Chinar Mega Mall, Chinar Fortune City, Hoshangabad Rd., Bhopal-462026, Madhya Pradesh, India, Tel: +91-755-6660006; E-mail: publication@trivedisrl.com

Received July 06, 2015; **Accepted** July 16, 2015; **Published** July 23, 2015

Citation: Trivedi MK, Patil S, Mishra RK, Jana S (2015) Thermal and Physical Properties of Biofield Treated Bile Salt and Proteose Peptone. J Anal Bioanal Tech 6: 256 doi:10.4172/2155-9872.1000256

objects around the Globe. The objects always receive the energy and responding into useful way that is called biofield energy and the process is known as biofield treatment. Recently, biofield energy has shown significant effect on structural, crystalline and thermal properties of various metals, ceramics and carbon allotropes [14-17].

Mr. Mahendra K. Trivedi is known to transform the properties of various living and non-living things under controlled experiments using his unique biofield energy. Biofield treatment had substantially changed the atomic, crystalline, surface properties of various materials. The biofield had significantly changed the overall productivity and quality in the field of agriculture and biotechnology [18-21]. Additionally, biofield has shown excellent results in improving antimicrobial susceptibility, and alteration of biochemical reactions, as well as induced alterations in characteristics of pathogenic microbes [22-24]. The biofield had also caused an increase in growth and anatomical characteristics of an herb *Pogostemon cablin* that is commonly used in perfumes, in incense/insect repellents, and alternative medicine [25].

In the present study, the influence of biofield treatment on physicochemical properties of BS and PP were studied with the aid of different methods like particle size analyzer (PSA), Brunauer-Emmett-Teller (BET) analysis, differential scanning calorimetry (DSC), X-ray diffraction (XRD) studies, and thermogravimetric analysis (TGA).

Experimental

Materials and methods

The Bile salt and Proteose peptone were procured from Hi Media Laboratories Pvt. Ltd., Mumbai, India. Each material was divided into two parts; one was kept as a control sample, while the other was subjected to Mr. Trivedi's biofield treatment and coded as treated sample (T). The treatment group (T) was in sealed pack and handed over to Mr. Trivedi for biofield treatment under laboratory condition. Mr. Trivedi provided the treatment through his energy transmission process to the treated group without touching the sample.

Characterization

Particle size analysis: The average particle size and particle size distribution were analyzed by using Sympetac Helos-BF Laser Particle Size Analyzer with a detection range of 0.1 micrometer to 875 micrometer. Average particle size d_{50} and d_{99} (size exhibited by 99% of powder particles) were computed from laser diffraction data table. The d_{50} and d_{99} values were calculated by the following formula:

Percentage change in d_{50} size=100 × (d_{50} treated-d_{50} control)/d_{50} control

Percentage change in d_{99} size=100 × (d_{99} treated-d_{99} control)/d_{99} control

Surface area analysis: The surface area of BS and PP were characterized using surface area analyzer, SMART SORB 90 BET, which had a detection range of 0.1-100 m^2/g.

Differential scanning calorimetry (DSC) study: The control and treated samples (BS and PP) were analyzed using a Pyris-6 Perkin Elmer DSC on a heating rate of 10°C/min under air atmosphere.

X-ray diffraction (XRD) study: XRD of BS and PP (control and treated) powders were analyzed by using Phillips Holland PW 1710 X-ray diffractometer system. The wavelength of the radiation was 1.54056 angstrom. The data was obtained in the form of 2θ versus intensity (a.u) chart. The obtained data was used for calculation of crystallite size using the following formula.

Crystallite size=kλ/b Cos θ

Where λ is the wavelength and k is the equipment constant (0.94).

Thermogravimetric analysis-Differential thermal analysis (TGA-DTA): Thermal stability of control and treated samples (BS and PP) were analyzed using Mettler Toledo simultaneous TGA and Differential thermal analyzer (DTA). The samples were heated from room temperature to 400°C with a heating rate of 5°C/min under air atmosphere.

Results and Discussion

Particle size and surface area analysis

The average particle size (d_{50}) and particle size (d_{99}) of the organic products were computed from particle size distribution graph and the data are presented in Figures 1 and 2. The average particle size (d_{50}) of treated BS (13.24 µm) was enhanced as compared to control sample (12.13 µm) (Figure 1). Similarly, the d_{99} value of the treated BS (121.65 µm) showed increase as compared to control sample (88.77 µm). The calculated percentage change in average particle size (d_{50}) was 9.2% and d_{99} value was 37%. This substantial increase in particle size of the treated BS may be due to biofield treatment which may be caused fracture in the particles hence the powder may not have specific boundaries that can be led to particles agglomeration and increased particle size. It is assumed that bigger treated microparticles may be useful in designing drug delivery systems. Many reports suggested that higher water uptake of organic products such as rice bran, mainly depends on its particle size [26-28]. It was envisaged that larger size particles take up more water as compared to smaller particles [29]. Albers *et al.*, in a research study showed that water absorption decreased with decreasing particle size [26]. Hence, bigger microparticles are likely to show more water uptake and this property can be used for controlled release of drugs. The drugs can be released from swellable microparticle through diffusion, degradation or both depending on the level of swelling and solubility of the drug [30]. Therefore, the treated BS could be interesting choice for drug delivery systems.

The PP also showed increase in d_{50} (14.4 µm) and d_{99} (130.09 µm) as compared to control PP sample (d_{50}; 13.42, d_{99}; 107.58) (Figure 1). The percentage change in d_{50} and d_{99} values was 7.3% and 20.9 % respectively (Figure 2). It is assumed that aggregation due to biofield treatment might cause the particles to come together and form bigger

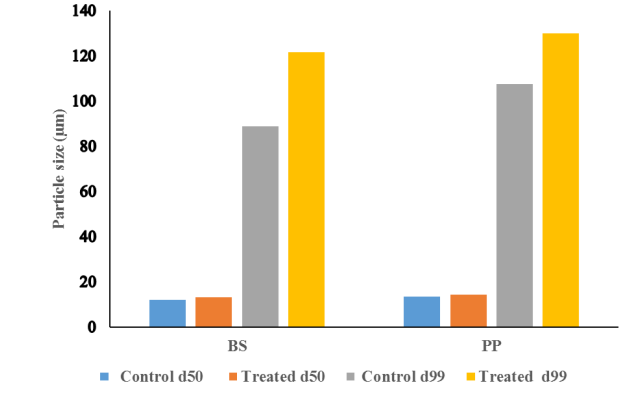

Figure 1: Particle size (d_{50} and d_{99}) distribution of bile salt (BS) and proteose peptone (PP) (control and treated).

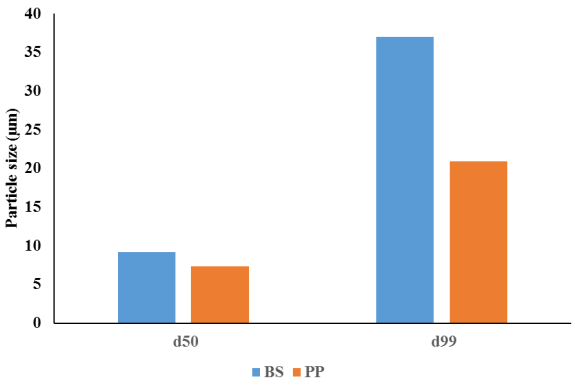

Figure 2: Percentage change in particle size of bile salt (BS) and proteose peptone PP (control and treated).

microparticles. It was previously described that proteins have stronger tendency of forming aggregates. They can form self-aggregates in a number of ways such as formation of structural complexes, multimeric native states with metal complexation [31-33]. These proteins have sufficiently strong inter-protein interactions [34] which induce formation of bigger aggregates. It is postulated that biofield may be interacted with protein assembly of PP and caused bigger microparticle formation.

Surface area of BS and PP was measured and results are presented in Table 1. The surface area of control BS was 0.63 m^2/g. However, after treatment it was decreased slightly *i.e.* up to 0.62 m^2/g. The percentage decrease in surface area was by 1.59% in treated BS sample as compared to control. The minimal decrease in surface area was due to increase in particle size of treated BS [35,36]. Contrarily, the treated PP (1.08 m^2/g) showed increase in surface area as compared to control (1.00 m^2/g). The percentage increase in surface area was 8% in the treated PP with respect to control. It is assumed that biofield energy might cause formation of sharp edges or pore formation over particle surface which increased the resultant surface area.

DSC studies

DSC thermogram of control and treated BS are presented in Figure 3. The DSC thermogram of control BS showed broad endothermic peak at 128°C which was due to melting temperature of the sample. DSC of treated BS showed endothermic peak at 232°C which was probably associated with melting and hydration of the hydrophilic head in BS structure. The increase in melting temperature may be correlated with high thermal stability of treated BS. In BS the increase in temperature raises the critical micelle concentration; however further increase in temperature decreases the critical micelle concentration. At a fixed temperature the critical micelle concentration value of BS is controlled by balanced interaction of two forces namely van der Waals forces between the hydrophobic alkyl groups that stabilizes the micelles and opposing hydration of hydrophilic group that deny the formation of micelles. These two opposite factors are to be considered in order to understand this behavior, *viz* increase in temperature elevates the dehydration of head group (resulting in increased hydrophobic nature of the molecules) and thermal stability of the BS molecules [37]. Hence, it is postulated that thermal along with biofield energy might be acted at BS molecules which enhanced the hydrophobic nature and thermal stability.

DSC thermogram of control and treated PP are shown in Figure 4. The control PP showed an endothermic peak due to absorbed water at 122°C and another endothermic inflexion was observed at around 300°C which was due to melting temperature and thermal denaturation of the control sample. DSC thermogram of treated sample exhibited a broad endothermic peak at 175°C. Researchers have found that the major endothermic peak observed (from 0 to 180°C) in case of soy protein, gelatin, sodium casein and corn gluten meal has been attributed to loss of residual water or hydrogen bond disruption between protein molecules [38-41]. Another endothermic peak was observed at 290°C in the treated PP which was probably due to thermal denaturation and melting temperature of the protein. The control PP showed an exothermic temperature peak at around 267°C. However, the DSC thermogram of treated PP showed (Figure 4) an exothermic transition at 278°C. Tang *et al.* during their studies on heat induced aggregation and denaturation of soy proteins observed much lower exothermic peaks (150°C) [38]. It is presumed that exothermic peak might be increased due to biofield treatment. The native confirmation of proteins is mainly maintained by its inherent hydrogen bonding and electrostatic interactions, whereas thermal stability is closely related to hydrophobic interactions. If the hydrophilic interactions retaining the tertiary structure of protein are ruptured by heating, hydrophobic regions initially hidden inside the proteins will be exposed to the protein surface and subordinate with other hydrophobic protein molecules to form aggregates. Hence, in this study the exothermic peak could be attributed to the protein aggregation [42,43]. Additionally, the increase in exothermic peak may be due biofield energy which raised the treated PP aggregation temperature.

XRD studies

XRD diffractogram of control and treated BS are illustrated in Figure 5. The XRD diffractogram of control BS showed presence of broad as well as intense peak. The control sample showed crystalline peaks at 2θ equals to 31.61°, 45.40°, 56.42°, 66.12° and 75.26°. The control BS showed a broad peak at 2θ equals to 11.1° which was due to amorphous nature. These XRD peaks showed presence of both crystalline as well as amorphous regions in the control BS (Figure 5). The treated BS also displayed similar XRD peaks at 2θ equals to 27.2°, 31.63°, 45.39°, 56.45°, 66.14° and 75.10°. The result showed a minimal reduction in the intensity of the XRD peaks in the treated BS which may be due to decrease in crystallinity of the sample.

XRD diffractogram of control and treated PP are shown in Figure 6. The XRD of control sample showed an amorphous nature which was confirmed by a broad peak at around 2θ equals to 14.48° and 23°. However, the treated PP showed (Figure 6) XRD peaks at around 2θ equals to 28.39° and 32.71° which showed no significant change in amorphous nature of the treated PP after biofield treatment.

TGA studies

TGA was used to get further insights about the thermal stability of the control and treated samples (BS and PP). The TGA thermogram of BS (control and treated) are presented in Figures 7 and 8. The TGA thermogram of control BS exhibited one step thermal degradation. The thermal degradation commenced at 80°C and continued up to 130°C. The sample had lost 3.28% of its total original weight during this process. This thermal event was probably associated with

Sample	Control (m^2/g)	Treated (m^2/g)	%Change in surface area
Bile salt	0.63	0.62	-1.59
Proteose peptone	1.00	1.08	8.00

Table 1: Surface area analysis of bile salt and proteose peptone.

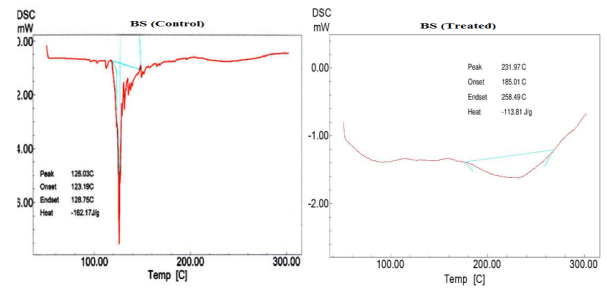

Figure 3: DSC thermogram of control and treated bile salt.

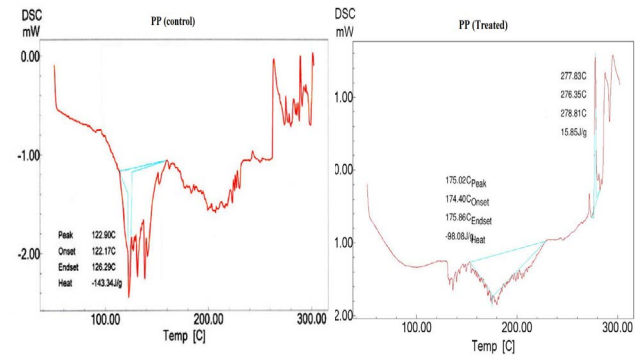

Figure 4: DSC thermogram of control and treated proteose peptone.

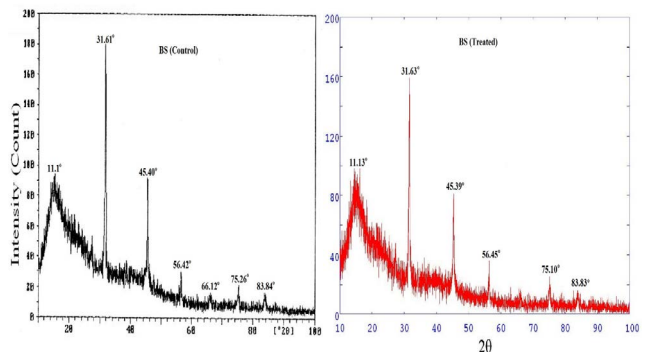

Figure 5: XRD diffractogram of control and treated bile salt.

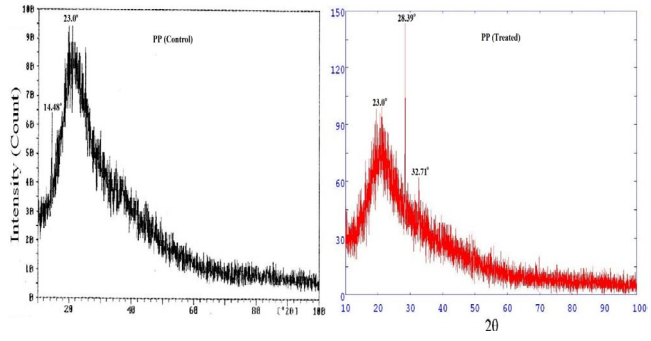

Figure 6: XRD diffractogram of control and treated proteose peptone.

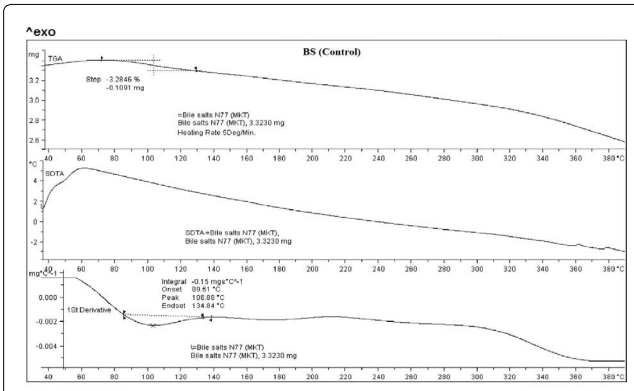

Figure 7: TGA thermogram of bile salt (Control).

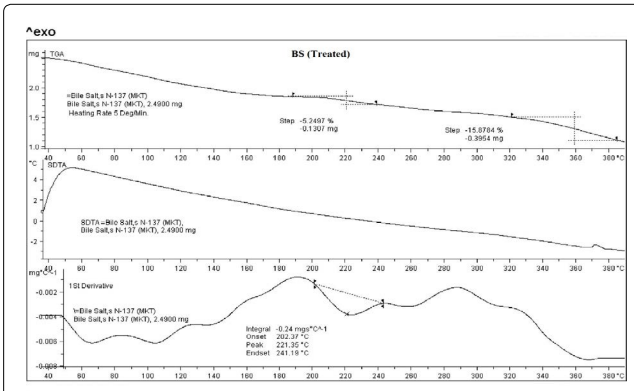

Figure 8: TGA thermogram of bile salt (Treated).

elimination of water or dehydration of the control sample (Figure 7). The derivative thermogravimetry (DTG) thermogram of control sample exhibited maximum thermal degradation at 106°C. Whereas the treated BS sample showed two step thermal degradation process. The first step commenced at around 190°C and terminated at around 240°C. The second thermal degradation event was commenced at 320°C and terminated at around 390°C. Major sample weight loss was observed during this process (15.87%). DTG thermogram of treated BS showed (Figure 8) maximum thermal decomposition step at 221°C which was higher as compared to control sample (106°C). The DTA thermogram of control and treated BS did not show any changes in the respective thermograms. However, the comparison of the DTG peaks confirmed that thermal stability of treated BS was enhanced after biofield treatment as compared to control sample [37].

TGA thermogram of control and treated PP are depicted in Figures 9 and 10. TGA thermogram of control PP showed two step thermal degradation. The first step thermal degradation started at 190°C and terminated at 230°C. However the second thermal degradation commenced at 260°C and terminated at 310°C (Figure 9). The control sample lost -9.15% and -9.84% weight respectively from the sample. DTG thermogram showed two peaks which were mainly due to initial decomposition temperature (205°C) and maximum thermal decomposition temperature (283°C) of the control sample. The TGA thermogram of treated PP also showed two step thermal degradation pattern. The first step thermal degradation started at 172°C and terminated at 259°C. Thereafter the second step was observed at 273°C and thermal degradation stopped at 371°C. During this thermal process the treated sample lost -18.28% and -21.70% of its weight.

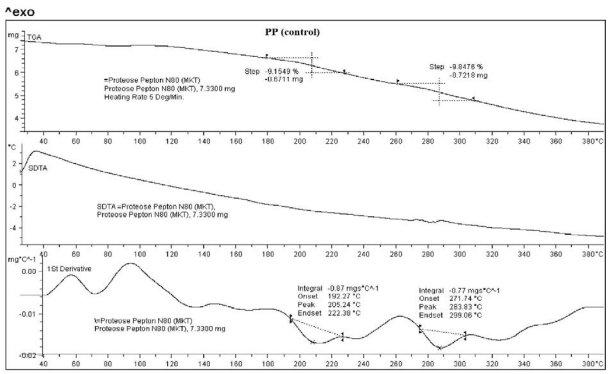

Figure 9: TGA thermogram of proteose peptone (Control).

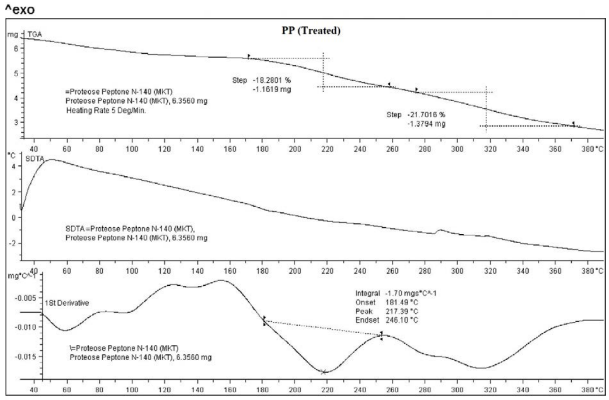

Figure 10: TGA thermogram of proteose peptone (Treated).

The DTG of treated PP showed (Figure 10) a decrease in maximum thermal decomposition temperature and it was observed at 217°C. This decrease in DTG peak could be due to decrease in thermal stability of treated PP as compared to control. DTA showed no changes in the thermal pattern of control and treated PP.

Conclusion

This research study has evaluated the influence of biofield treatment on thermal and physical properties of BS and PP. The treated BS showed increase in particle size (d_{50} and d_{99}) as compared to control which might be due to fracturing of internal boundaries in the particles caused by biofield treatment. The treated PP also showed increase in particle size with respect to control; possibly due to biofield treatment and protein aggregation. Additionally, biofield treatment showed significant alteration in thermal nature of the treated samples. Based on the results the biofield treated BS and PP could be used in drug delivery systems. Further, Circular dichroism spectroscopic and Scanning electron microscopy/Transmission electron microscopy studies could be carried out to get further depth insights about thermal stability and aggregation nature of these treated organic products.

Acknowledgement

The authors would like to thank all the laboratory staff of MGV Pharmacy College, Nashik for their assistance during the various instrument characterizations. We thank Dr. Cheng Dong of NLSC, institute of physics, and Chinese academy of sciences for permitting us to use PowderX software for analyzing XRD results.

References

1. Mukhopadhyay S, Maitra U (2004) Chemistry and biology of bile acids. Curr Sci 87: 1666-1683.
2. Bauer E, Jakob S, Mosenthin R (2005) Principles of Physiology of Lipid Digestion. Asian Australas J Anim Sci 18: 282-295.
3. Cabral DJ, Small DM (1989) Physical chemistry of bile: Handbook of Physiology. American Physiology Society, Bethesda, USA.
4. Hofmann AF, Small DM (1967) Detergent properties of bile salts: correlation with physiological function. Annu Rev Med 18: 333-376.
5. Madenci D, Egelhaaf SU (2010) Self-assembly in aqueous bile salt solutions. Curr Opin Colloid Interface Sci 15: 109-115.
6. Holm R, Müllertz A, Mu H (2013) Bile salts and their importance for drug absorption. Int J Pharm 453: 44-55.
7. Andrews AT, Alichanidis E (1983) Proteolysis of caseins and the proteose-peptone fraction of bovine milk. J Dairy Res 50: 275-290.
8. Paquet D (1989) Literature review: the proteose peptones milk fraction. Lait 69: 1-21.
9. Andrews AT (1983) Proteinases in normal bovine milk and their action on caseins. J Dairy Res 50: 45-55.
10. Eigel WN, Butler JE, Ernstrom CA, Farrell Jr HM, Harwalker VR, et al. (1984) Nomenclature of proteins of cows' milk: fifth revision. J Dairy Sci 67: 1599-1631.
11. Kaminogawa S, Mizobuchi H, Yamauchi K (1972) Comparison of bovine milk protease with plasmin. Agric Biol Chem 36: 2163-2167.
12. Myers R (2003) The basics of chemistry. Greenwood Press, Westport, Connecticut, USA.
13. Movaffaghi Z, Farsi M (2009) Biofield therapies: biophysical basis and biological regulations? Complement Ther Clin Pract 15: 35-37.
14. Trivedi MK, Patil S, Tallapragada RM (2013) Effect of biofield treatment on the physical and thermal characteristics of vanadium pentoxide powders. J Material Sci Eng S11: 001.
15. Trivedi MK, Patil S, Tallapragada RM (2013) Effect of biofield treatment on the physical and thermal characteristics of silicon, tin and lead powders. J Material Sci Eng 2: 125.
16. Trivedi MK, Patil S, Tallapragada RM (2014) Atomic, crystalline and powder characteristics of treated zirconia and silica powders. J Material Sci Eng 3: 144.
17. Trivedi MK, Patil S, Tallapragada RMR (2015) Effect of biofield treatment on the physical and thermal characteristics of aluminium powders. Ind Eng Manag 4: 151.
18. Shinde V, Sances F, Patil S, Spence A (2012) Impact of biofield treatment on growth and yield of lettuce and tomato. Aust J Basic Appl Sci 6: 100-105.
19. Sances F, Flora E, Patil S, Spence A, Shinde V (2013) Impact of biofield treatment on ginseng and organic blueberry yield. Agrivita J Agric Sci 35: 22-29.
20. Lenssen AW (2013) Biofield and fungicide seed treatment influences on soybean productivity, seed quality and weed community. Agricultural Journal 8: 138-143.
21. Altekar N, Nayak G (2015) Effect of biofield treatment on plant growth and adaptation. J Environ Health Sci 1: 1-9.
22. Trivedi MK, Patil S (2008) Impact of an external energy on *Staphylococcus epidermis* [ATCC - 13518] in relation to antibiotic susceptibility and biochemical reactions - An experimental study. J Accord Integr Med 4: 230-235.
23. Trivedi MK, Patil S (2008) Impact of an external energy on *Yersinia enterocolitica* [ATCC - 23715] in relation to antibiotic susceptibility and biochemical reactions: An experimental study. Internet J Alternative Med 6: 2.
24. Trivedi MK, Bhardwaj Y, Patil S, Shettigar H, Bulbule A (2009) Impact of an external energy on *Enterococcus faecalis* [ATCC - 51299] in relation to antibiotic susceptibility and biochemical reactions – An experimental study. J Accord Integr Med 5: 119-130.
25. Patil SA, Nayak GB, Barve SS, Tembe RP, Khan RR (2012) Impact of biofield treatment on growth and anatomical characteristics of Pogostemon cablin

(Benth.). Biotechnology 11: 154-162.

26. Albers S, Muchova Z, Fikselova M (2009) The effects of different treated brans additions on bread quality. Scientia Agriculturae Bohemica 40: 67-72.
27. Auffret A, Ralet MC, Guillon F, Barry JL, Thibault JF (1994) Effect of grinding and experimental conditions on the measurement of hydration properties of dietary fibers. LWT-Food Sci Technol 27: 166-172.
28. Zhang DC, Moore WR (1997) Effect of wheat bran particle size on dough rheological properties. J Sci Food Agr 74: 490-496.
29. Robertson JA, Eastwood MA (1981) An investigation of the experimental conditions which could affect water-holding capacity of dietary fiber. J Sci Food Agr 32: 819-825.
30. Omidian H, Park K (2008) Swelling agents and devices in oral drug delivery. J Drug Del Sci Tech 18: 83-93.
31. Midelfort KS, Wittrup KD (2006) Context-dependent mutations predominate in an engineered high-affinity single chain antibody fragment. Protein Sci 15: 324-334.
32. Hooper NM (1994) Families of zinc metalloproteases. FEBS Lett 354: 1-6.
33. Wiseman RL, Powers ET, Kelly JW (2005) Partitioning conformational intermediates between competing refolding and aggregation pathways: insights into transthyretin amyloid disease. Biochemistry 44: 16612-16623.
34. Amin S, Barnett GV, Pathak JA, Roberts CJ, Sarangapani PS (2014) Protein aggregation, particle formation, characterization & rheology. Curr Opin Colloid Interface Sci 19: 438-449.
35. Mennucci B, Martinez JM (2005) How to model solvation of peptides? Insights from a quantum-mechanical and molecular dynamics study of N-methylacetamide. I. Geometries, infrared, and ultraviolet spectra in water. J Phys Chem B 109: 9818-9829.
36. Bendz D, Tuchsen PL, Christensen TH (2007) The dissolution kinetics of major elements in municipal solid waste incineration bottom ash particles. J Contam Hydrol 94: 178-194.
37. Rub MA, Sheikh MS, Asiri AM, Azum N, Khan A, et al. (2013) Aggregation behaviour of amphiphilic drug and bile salt mixtures at different compositions and temperatures. J Chem Thermodynamics 64: 28-39.
38. Tang CH, Chen Z, Li L, Yang XQ (2006) Effects of transglutaminase treatment on the thermal properties of soy protein isolates. Food Res Int 39: 704-711.
39. Bell LN, Touma DE (1996) Glass transition temperatures determined using a temperature cycling differential scanning calorimeter. Food Sci 61: 807-810.
40. Di Gioia L, Cuq B, Guilbert S (1999) Thermal properties of corn gluten meal and its proteic components. Int J Biol Macromol 24: 341-350.
41. Tang CH, Yang XQ, Chen Z, Wu H, Peng ZY (2005) Physicochemical and structural characteristics of sodium caseinate biopolymers induced by microbial transglutaminase. J Food Biochem 29: 402-421.
42. Arntfield SD, Murray ED (1981) The influence of processing parameters on food protein functionality I. Differential scanning calorimetry as an indicator of protein denaturation. Can Inst Food Sci Technol J 14: 289-294.
43. Privalov PL (1982) Stability of proteins. Proteins which do not present a single cooperative system. Adv Protein Chem 35: 1-104.